

Figure legends:

Supplemental Figure 1: Cardiovascular abnormalities in MFS mice. **(A)** TAA; On the left are representative Echo images of the parasternal long axis of *Fbn1*^{+/+} and *Fbn1*^{mgR/mgR} mice with highlights of the aortic root (yellow bar; AoR) and proximal ascending aorta (red bar; AsAo). On the right are the average diameters of the same anatomical sites in *Fbn1*^{+/+} (black) and *Fbn1*^{mgR/mgR} (gray) mice. Asterisks indicate statistically significant differences ($p < 0.05$; $n = 8$ per genotype) and bars indicate mean \pm SD. **(B)** Valvular disease: aortic and mitral valve regurgitation (AV and MV, respectively) as seen by parasternal Echo; regurgitation is represented as a blue backwards flow.

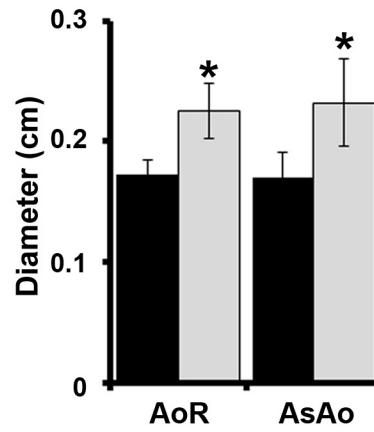
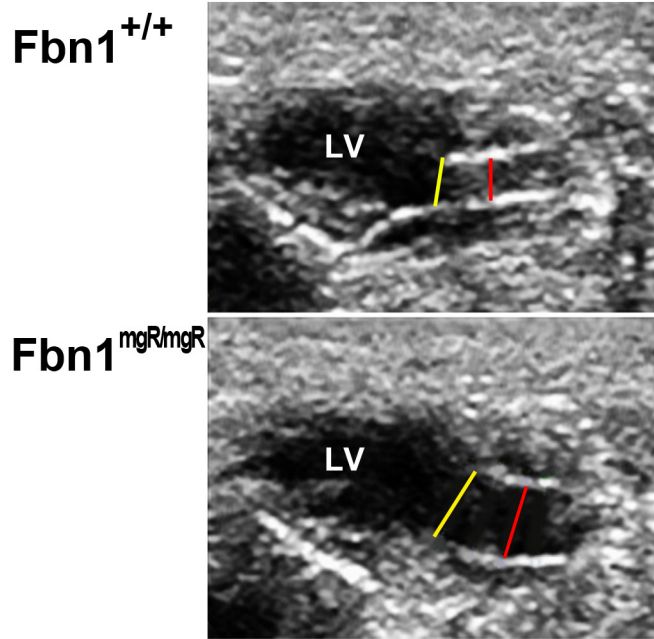
Supplemental Figure 2: Characterization of conditionally inactivated *Fbn1* mice. **(A)** Illustrative whole mount X-gal staining of neonatal hearts of the indicated genotypes with cross-section of myocardial tissue shown below; scale bar = 50 μm . **(B)** Bar graphs summarizing qPCR estimates of *Fbn1* transcript levels in cardiomyocytes and cardiac fibroblasts isolated from newborn mice of the indicated genotypes. Transcript levels in cells from conditional mutant mice is shown together with those from the respective parental mutant mice and both groups are expressed relative to *Fbn1*^{+/+} levels (100%); values from *Fbn1*^{mgR/mgR} cardiomyocytes are included as a reference. Asterisks indicate statistically significant differences ($p < 0.05$; $n = 5$ per all genotypes but $n = 18$ for *Fbn1* ^{α MHC-/-} mice) and bars indicate mean \pm SD. **(C)** Representative images of *Fbn1*^{+/+} and myxomatous mitral valve (black arrowhead; scale bar = 50 μm) or TAA (yellow

arrowhead; scale bar = 1mm) in 6-week-old *Fbn1*^{Col2^{-/-}} and *Fbn1*^{Wnt1^{-/}/mgR} mice respectively. (D) Cardiac size in 6-week-old *αMHC-Cre* transgenic mice evaluated according to the indicated criteria. Black and gray bars refer to *αMHC-Cre*⁻ and *αMHC-Cre*⁺ mice, respectively (n≥5 per genotype).

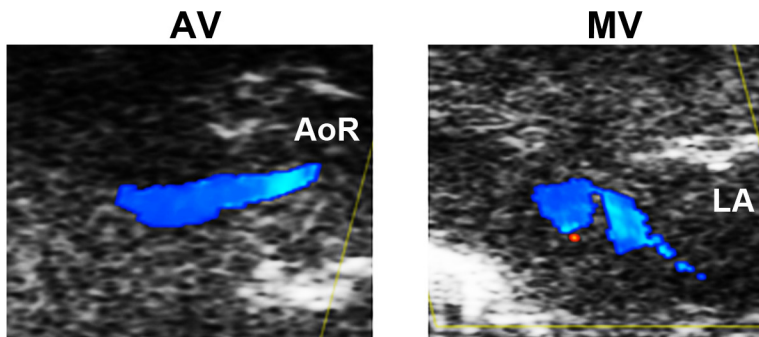
Supplemental Figure 3: Ultrastructure of fibrillin-1 deficient pericellular matrix. Representative electron microscopy images of myocardial cross-sections from P16 *Fbn1*^{+/+} and *Fbn1*^{-/-} mice with arrows in the magnified images on the right pointing to the BM-associated pericellular matrix. Scale bar = 1μM.

Supplemental Figure 4: TGFβ antagonism in *Fbn1*^{αMHC^{-/-}} mice. Representative hearts collected from 3-month-old *Fbn1*^{+/+}, untreated *Fbn1*^{αMHC^{-/-}}, and 1D11-treated *Fbn1*^{αMHC^{-/-}} mice (upper panel). Below are evaluations of the same animals for the indicated parameters of cardiac function or size. Asterisks indicate statistically significant differences compared to *Fbn1*^{+/+} mice (p<0.05; n≥5 per genotype) and bars indicate mean ± SD, ANOVA p < 0.002.

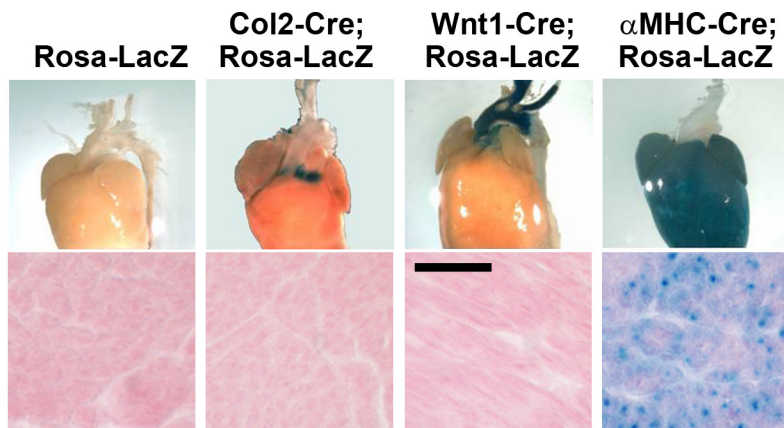
A



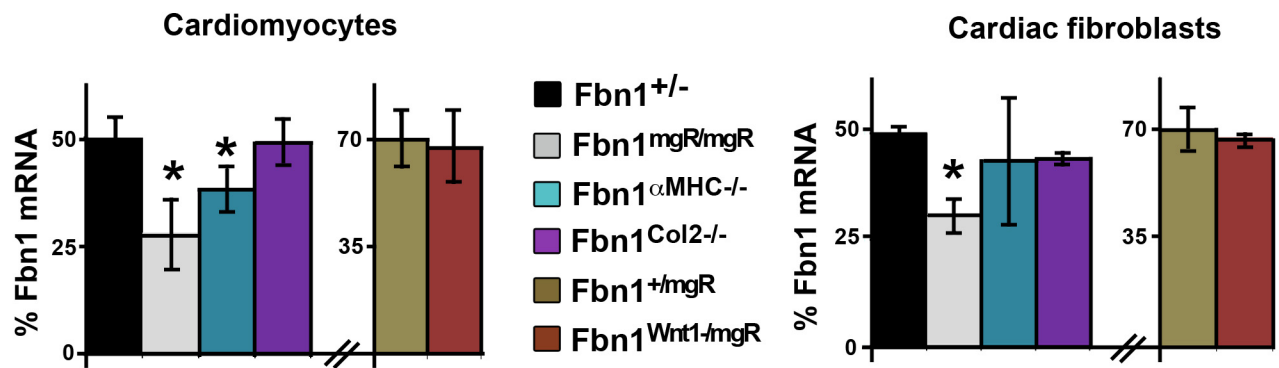
B



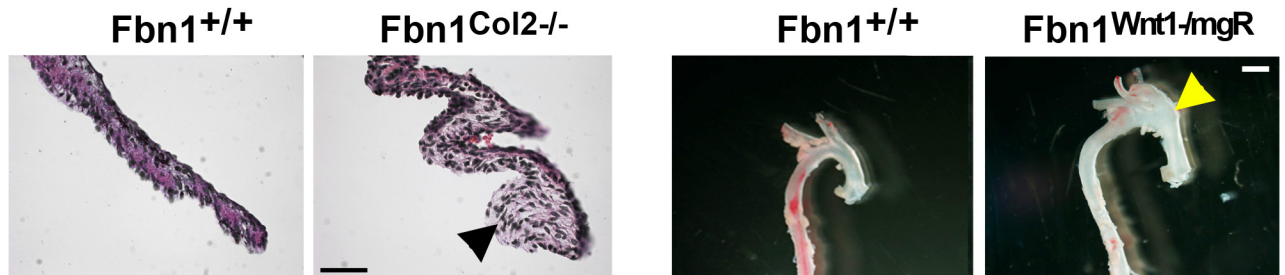
A



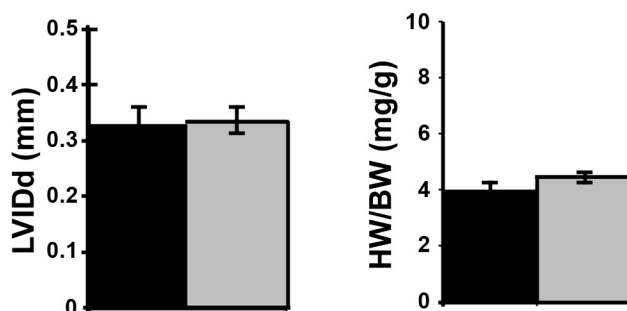
B



C

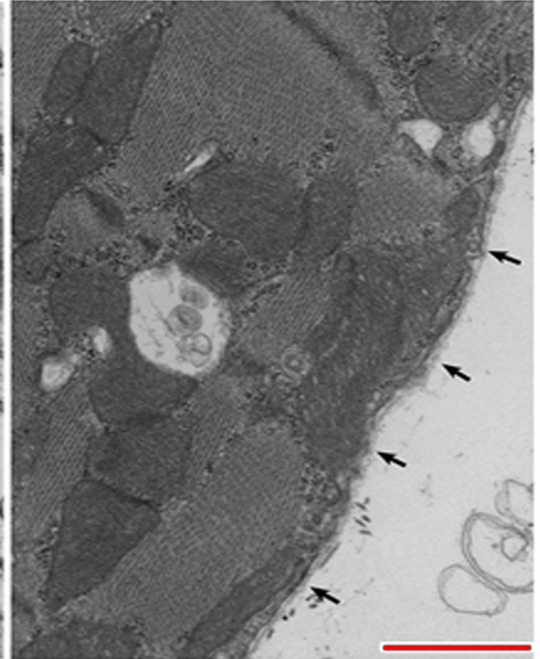
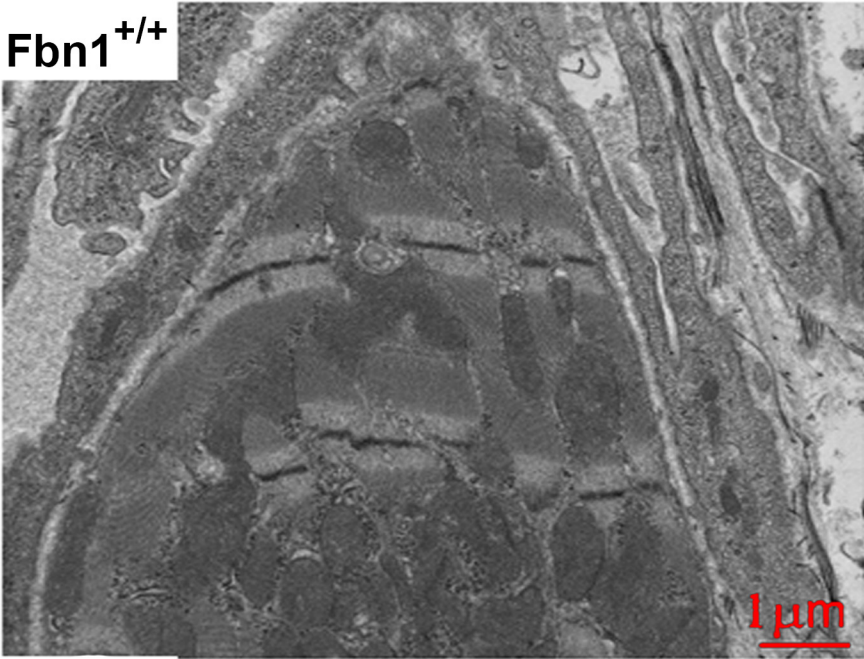


D

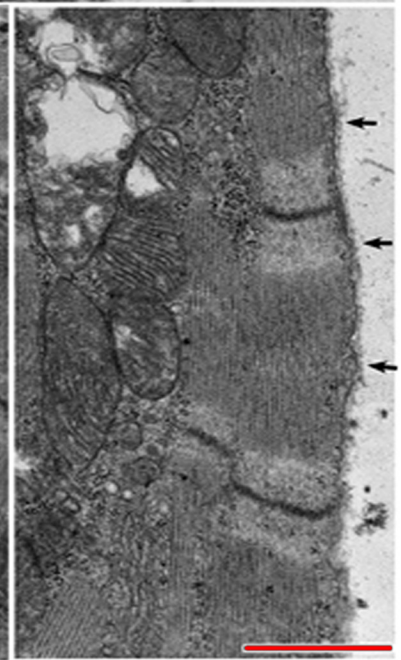
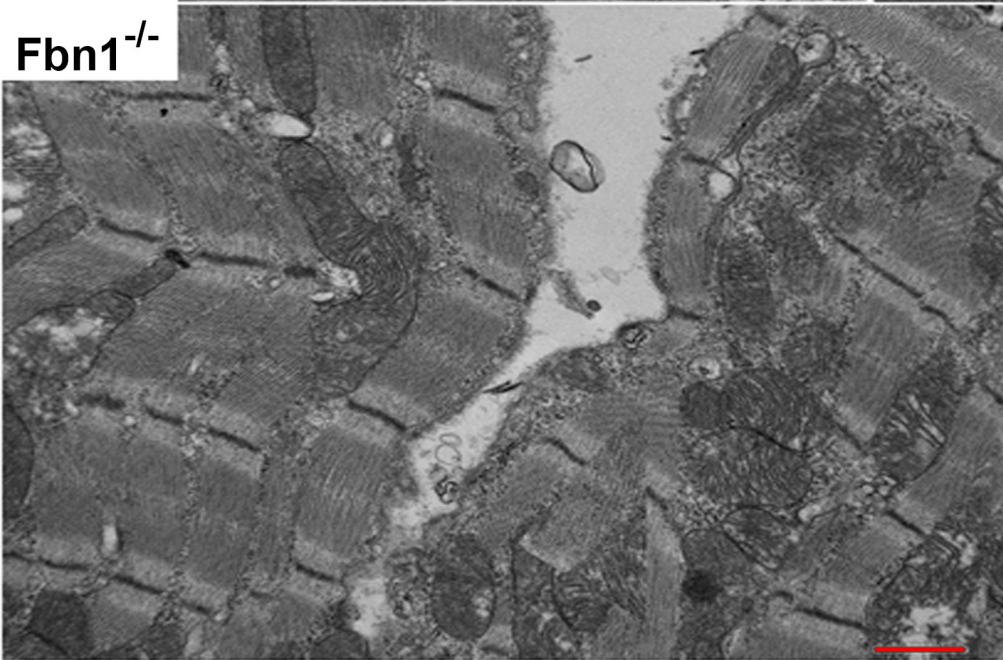


Supplemental Fig 3

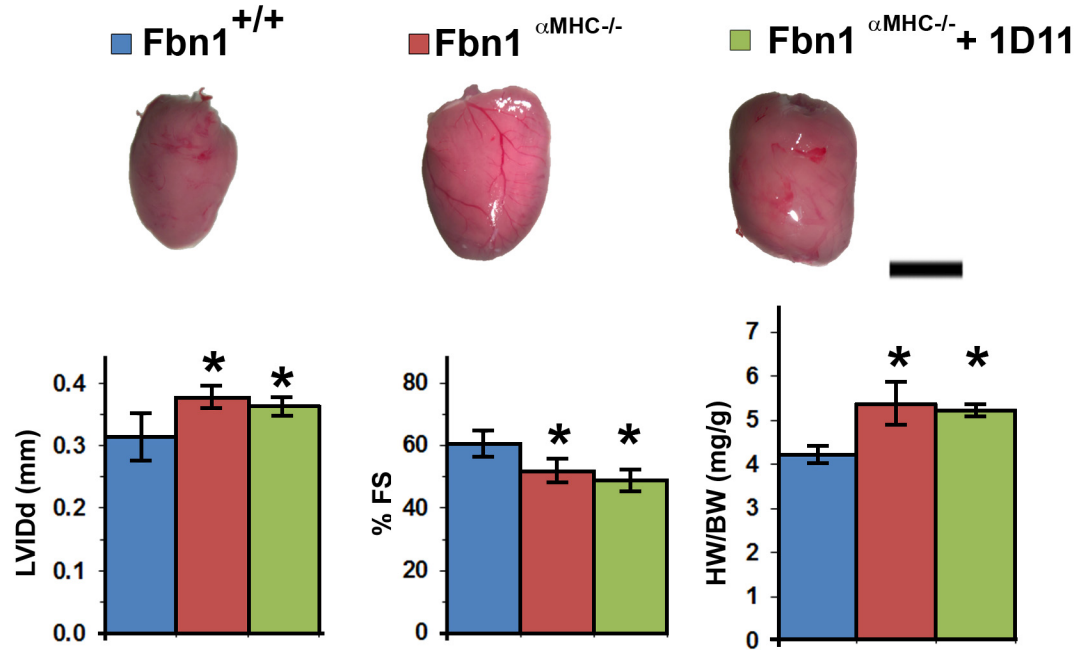
Fbn1^{+/+}



Fbn1^{-/-}



Supplemental Fig 4



GenTAC Participating Centers and Investigators

Johns Hopkins University: Williams Ravekes, MD, Harry C. Dietz, MD, Kathryn W. Holmes, MD, Jennifer Habashi, MD, Kira Lurman, RN.

University of Texas-Houston: Dianna M. Milewicz, MD, PhD, Siddharth K. Prakash, MD, PhD, Meghan A. Terry.

Baylor College of Medicine: Scott A. LeMaire, MD, Shaine A. Morris, MD, Irina Volguina, PhD.

Oregon Health and Science University: Cheryl L Maslen, PhD, Howard K. Song, MD, PhD, Michael Silberbach, MD, Carrie Farrar

University of Pennsylvania: Reed E. Pyeritz, MD, PhD, Joseph E. Bavaria, MD, Karianna Milewski, MD, PhD, Amber Parker

Weill Medical College of Cornell University: Richard B. Devereux, MD, Jonathan W. Weinsaft, MD, Mary J. Roman, MD, Tanya LaTortue.

The Queen's Medical Center: Ralph Shohet, MD, Fionna Kennedy

National Institute on Aging: Nazli McDonnell, MD, Ben Griswold

Medstar Health Research Institute: Federico M. Asch, MD

University of Michigan: Kim A. Eagle, MD

National Heart, Lung, and Blood Institute: H. Eser Tolunay, PhD, Patrice Desvigne-Nickens, MD, Mario P. Stylianou, PhD, Megan Mitchell, MPH

RTI International: Barbara L. Kroner, PhD, Liliana Preiss, MS, Tabitha Hendershot, Danny Ringer, Meg Crawford, Ryan Whitworth